Compounds with the Ir_3Ge_7 Structure Type: Interpenetrating Frameworks with Flexible Bonding Properties

Ulrich Häussermann,* Margareta Elding-Pontén, Christer Svensson, and Sven Lidin

Dedicated to the memory of Jeremy K. Burdett

Abstract: Reexamination of the E-rich (E = Ga, In) area of the binary systems Ni/Ga and Pd/In yielded the stoichiometric compounds Ni_3Ga_7 and Pd_3In_7 with the Ir_3Ge_7 structure type. The structure of the compounds was determined by single-crystal X-ray diffraction methods (space group $Im\bar{3}m$; Ni_3Ga_7: $a = 8.4285(6)$ Å, Pd_3In_7: $a = 9.4323(2)$ Å; $Z = 4$). The existence of the nonstoichiometric phases $NiGa_4$ and $PdIn_3$ reported earlier could not be confirmed and it is assumed that Ni_3Ga_7 and Pd_3In_7 represent the most E-rich compounds in their respective systems. The remarkable Ir_3Ge_7 structure consists of two equivalent interpenetrating frameworks built from cubes and square antiprisms. Its chemical bonding motifs were analysed by ab initio linear muffin-tin orbital (LMTO) and semiempirical tight-binding extended Hückel band-structure calculations. It was found that the valence electron concentration plays a crucial role in the structural stability of the Ir_3Ge_7 type and that, in the case of strong dp bonding between transition metal and E component, semiconducting representatives can occur. We suggest that the width of the band gaps is tunable by the choice of constituent elements in ternary and quarternary compounds with the Ir_3Ge_7 structure.

Keywords: bond theory · density functional calculations · intermetallic phases · semiempirical calculations · solid-state structures

Introduction

Systems consisting of metametallic or semimetallic p-block elements E (Ga – In, Ge – Sn, As – Sb) and an electropositive counterpart (i.e. alkali and/or alkaline earth metals) have been the subject of extensive research for many years, which has yielded a myriad of compounds and structures.[1,2] Most of these compounds can be classified as Zintl phases, and their distinctive characteristic is the occurrence of covalently bonded polyanionic substructures formed by the E atoms. The electronic structure of the sp-bonded polyanions can be simply rationalised by electron counting schemes as the $(8-n)$ rule for two-electron – two-centre-bonded frameworks or Wade's rules for multicentre-bonded deltahedral cluster entities.[3]

When the electropositive component is exchanged for a transition metal T the chemical bonding picture changes dramatically; the clear relationship between electron count and geometrical structure prevalent in Zintl phases is lost in compounds T_mE_n. Considering E-rich systems, the p-block elements still exhibit a strong tendency to form homonuclear bonds, but additionally the interactions of the d orbitals of the T metals must be taken into account. Thus there is an interplay of dp and sp bonding in these compounds, leading to a more complex bonding situation. During our investigation of the E-rich parts of the systems Ni/Ga and Pd/In we obtained the compounds Ni_3Ga_7 and Pd_3In_7 with the Ir_3Ge_7 structure and realised that this remarkable structure type can accomodate both extremes, namely strongly dp-bonded and strongly sp-bonded representatives. Strong dp bonding occurs when the T component is chosen from among the earlier transition metals from the second or third transition series (Nb, Mo, Re). As a consequence of strong dp bonding a band gap is opened at or close to the Fermi level and semiconducting compounds can be obtained. When the d orbitals of the T component are very contracted, as for example in Ni, a sp-bonded substructure of E atoms emerges which resembles the E substructures in Zintl phases. In this article we report on the synthesis and structural determination of the compounds Ni_3Ga_7 and Pd_3In_7, and the analysis of the bonding motifs associated with the Ir_3Ge_7 structure type.

[*] Dr. U. Häussermann, Prof. S. Lidin
Department of Inorganic Chemistry, Stockholm University
10691 Stockholm (Sweden)
Fax: (+46) 8-152187
E-mail: ulrich@inorg.su.se
Dr. M. Elding-Pontén, Dr. C. Svensson
Department of Inorganic Chemistry 2, Lund University
P.O. Box 124, 22100 Lund (Sweden)

 © WILEY-VCH Verlag GmbH, D-69451 Weinheim, 1998 0947-6539/98/0406-1007 $ 17.50+.25/0

Experimental Section

Synthesis: The compounds Ni_3Ga_7 and Pd_3In_7 were prepared from mixtures of the pure elements (Ni powder, puriss., Fluka; Pd powder, 99.9%, ABCR; Ga ingot, 99.9%, ABCR; In shot, 99.9%, Aldrich) containing 1 mmol transition metal and 10 mmol E element. The reactants were pressed into pellets and loaded into quartz ampoules, which were sealed under vacuum. Ni/Ga samples were heated to either 300° or 600 °C, Pd/In samples to 800 °C, for two days and then slowly cooled to room temperature at an approximate rate of 10 °h^{-1}. Excess E was dissolved with 4 M HCl. The highly crystalline products, which contained cube-shaped and tabular single crystals, were characterised by Guinier powder diagrams ($Cu_{K\alpha}$) and their composition analysed with the EDX (energy-disperse X-ray) method in a JEOL scanning electron microscope. The powder patterns for both systems revealed a cubic body-centred lattice consistent with the Ir_3Ge_7 structure type. In the case of the Ni/Ga products the powder patterns exhibited additional weak lines from traces of the compound Ni_2Ga_3 with the Ni_2Al_3 structure.

X-ray structure determination: Intensity data sets of suitable single crystals were collected at room temperature with $Mo_{K\alpha}$ radiation (graphite monochromator) on a Siemens SMART CCD diffractometer.[4] The data collection nominally covered a full sphere of reciprocal space. Combinations of five sets of exposures were used where each set had a different ϕ angle for the crystals and each exposure covered 0.3° in ω. The crystal-to-detector distance was 3.0 cm. The data reduction was performed with the program SAINT[5] and an empirical absorption correction with the program SADABS.[6] The space group $Im\bar{3}m$ was assigned on the basis of the systematic absences and the statistical analysis of the intensity distributions. Cell constants were obtained from a least-squares refinement of the setting angle of 46 (Ni_3Ga_7) and 50 (Pd_3In_7) centred reflections on a Huber four-circle diffractometer. The crystal structures were refined with the Ir_3Ge_7 structure as model by full-matrix least-squares refinement on F^2 (program SHELXL-93[7]) with the scattering factors of Ni/Ga and Pd/In, respectively. Some details of the single crystal data collections and refinements are listed in Table 1. Because of the similar scattering power of the atoms in the pairs Ni/Ga and Pd/In, the occurrence of T/E mixed occupancy positions in Ni_3Ga_7 and Pd_3In_7 cannot be totally excluded on the basis of the refinement results. However, the composition of the actual crystals was determined to be T_3E_7 by EDX analyses after the X-ray data had been collected. Therefore we concluded that the distribution of the T and E atoms corresponds to that in the structure type Ir_3Ge_7, which is also plausible from chemical considerations (see Results and Discussion, Section 2).

Table 1. Summary of crystal data for Ni_3Ga_7 and Pd_3In_7.

	Ni_3Ga_7	Pd_3In_7
crystal size [mm^3]	0.05 × 0.05 × 0.02	0.06 × 0.05 × 0.09
crystal system	cubic	cubic
space group	$Im\bar{3}m$ (No. 229)	$Im\bar{3}m$ (No. 229)
lattice constants [Å]	$a = 8.4285(6)$	$a = 9.4323(2)$
volume [$Å^3$]	598.76	839.18
Z	4	4
ρ_{calcd} [$g\,cm^{-3}$]	7.368	8.888
T [K]	295	295
λ [$Å^{-1}$]	0.71069 ($Mo_{K\alpha}$)	0.71069 ($Mo_{K\alpha}$)
absorption coeff [mm^{-1}]	40.02	25.02
$F(000)$	1204	1924
data collecn range, 2θ [°]	2–107.5	2–107.5
index range	$-18 \le h \le 18$	$-21 \le h \le 16$
	$-19 \le k \le 18$	$-15 \le k \le 21$
	$-19 \le l \le 10$	$-21 \le l \le 18$
measured reflns	11776	15393
unique reflns	402 ($R_{int}(F^2) = 0.071$)	552 ($R_{int}(F^2) = 0.059$)
reflns with $\|F\|^2 \ge 2\sigma(\|F\|^2)$	317	505
absorption corr	empirical (SADABS)	empirical (SADABS)
transmission ratio (max:min)	1.000:0.499	0.971:0.450
extinction corr[a]	$\chi = 0.0043(6)$	$\chi = 0.042(1)$
params refined	10	10
GoF on $\|F^2\|$	1.272	1.448
R values[b,c] [$\|F\|^2 \ge 2\sigma(\|F\|^2)$]	$R = 0.037$, $wR = 0.086$	$R = 0.026$, $wR = 0.052$
	$a = 0.043$, $b = 2.32$	$a = 0.02$, $b = 1.66$
R values (all data)	$R = 0.051$, $wR = 0.092$	$R = 0.030$, $wR = 0.053$
largest hole and peak, e/$Å^3$	−2.60 and 3.08	−2.75 and 1.40

[a] $F^* = F[1 + 0.002\chi F^2/\sin(2\theta)]^{1/4}$. [b] $R = [\Sigma(|F_o| - |F_c|)]/\Sigma|F_o|$.
[c] $wR = \{[\Sigma w(F_o^2 - F_c^2)^2]/\Sigma w(F_o^2)^2\}^{1/2}$. $w = [\sigma^2(|F_o|^2 + (aP)^2 + bP]^{-1}$.
$P = (F_o^2(\ge 0) + 2F_c^2)/3$.

Further details of the crystal structure investigations can be obtained from the Fachinformationszentrum Karlsruhe, D-76344 Eggenstein-Leopoldshafen (Germany) (Fax: (+49) 7247-808-666; e-mail: crysdata@fiz.karlsruhe.de) on quoting the depository numbers CSD-408313 (Ni_3Ga_7) and CSD-408314 (Pd_3In_7).

Theoretical calculations: The electronic structures of the compounds Mo_3Sb_7, Re_3As_7, Ir_3Ge_7, Ru_3Sn_7 and Ni_3Ga_7 were calculated self-consistently by means of the local density-functional approximation and the scalar relativistic linear muffin-tin orbital (LMTO) method in the atomic sphere approximation (ASA) including the combined correction (program TB-LMTO 4.6[8]). The exchange-correlation potential was parametrised according to von Barth and Hedin.[9] The TB-LMTO 4.6 program allows an automatic search of empty sphere (ES) positions and the determination of sphere radii.[10] The sum of the sphere volumes equalled the unit cell volumes and the maximum sphere overlap was below 15% for all possible sphere combinations. Table 2 summarises the structural parameters used in these calculations. The basis consisted of T and E s-, p-, d-, f-LMTOs for T = Mo, Ru, Re, Ir and E = Sn, Sb (T atom f- and E-atom d-, f-LMTOs downfolded), and of T and E s-, p-, d-LMTOs for T = Ni and E = Ga, Ge, As (E atom d-LMTOs downfolded). The reciprocal space integrations were performed with the tetrahedron method[11] from 72 irreducible k-points. For molecular orbital considerations and qualitative bonding analyses extended Hückel calculations were performed for the compounds Mo_3Sb_7 and Ni_3Ga_7 with a modified version of the program EHMACC[12] by using a 56 k-point mesh of the irreducible wedge. The Ni H_{ii} parameters were charge-iterated in order to obtain a better agreement of the Ni_3Ga_7 semiempirical and ab initio density of states (DOS). The resonance integrals were approximated by the Wolfsberg–Helmholtz formula $H_{ij} = {}^1/_2 KS_{ij}(H_{ii} + H_{jj})$ with $K = 1.75$. The calculational parameters are listed in Table 3.

Table 2. Structural data used in the LMTO calculations.

	Mo_3Sb_7	Re_3As_7	Ir_3Ge_7	Ru_3Sn_7	Ni_3Ga_7
a (Å)	9.5713	8.7162	8.735	9.332	8.4285
T	0.3425, 0, 0	0.3406, 0, 0	0.342, 0, 0	0.342, 0, 0	0.3406, 0, 0
r_T (Å)	1.5734	1.5192	1.4932	1.4967	1.3828
E1	0.25, 0, 0.5	0.25, 0, 0.5	0.25, 0, 0.5	0.25, 0, 0.5	0.25, 0, 0.5
r_{E1} (Å)	1.6620	1.4334	1.4623	1.6443	1.4102
E2	0.1624, x, x	0.1678, x, x	0.156, x, x	0.156, x, x	0.16125, x, x
r_{E2} (Å)	1.6225	1.4041	1.3905	1.5680	1.4600
ES1	0, 0, 0	0, 0, 0	0, 0, 0	0, 0, 0	0, 0, 0
r_{ES1} (Å)	1.4576	1.4902	1.3097	1.3017	1.2186
ES2	0, 0.2778, y	0, 0.2778, y	0, 0.2639, y	0, 0.2639, y	0, 0.2778, y
r_{ES2} (Å)	0.7902	0.7968	0.8190	0.8227	0.7376
ES3	0.3344, x, 0.1200	0.3438, x, 0.1199	0.3236, x, 0.1264	0.3135, x, 0.1231	0.3413, x, 0.1166
r_{ES3} (Å)	0.7605	0.7161	0.6865	0.6820	0.6712

Table 3. Parameters of the semiempirical calculations.

H_{ii} (eV), ζ_i	Mo_3Sb_7	Ni_3Ga_7
T d (dz)	−10.5, 4.540 (0.58988)	−10.132, 4.540 (0.57256)
	1.9 (0.58988)	1.9 (0.57256)
T s	− 8.34, 1.96	− 7.048, 1.96
T p	− 5.24, 1.9	− 3.515, 1.9
E s	−18.8, 2.323	−14.58, 1.77
E p	−11.7, 1.999	− 6.75, 1.55

© WILEY-VCH Verlag GmbH, D-69451 Weinheim, 1998
0947-6539/98/0406-1008 $ 17.50+.50/0 *Chem. Eur. J.* **1998**, *4*, No. 6

Results and Discussion

1. The compounds Ni_3Ga_7 and Pd_3In_7

The E-rich parts of the systems Ni/Ga and Pd/In have been the subject of several investigations in which structural analyses were performed with X-ray powder diffraction methods. In 1947 Hellner and Laves reported on the body-centred cubic phases '$NiGa_4$' ($a = 8.41$ Å) and '$PdIn_3$' ($a = 9.42$ Å), for which they proposed a γ-brass structure with defects,[13] and in a subsequent publication Hellner confirmed the existence of the phase '$NiGa_4$'.[14] More recently Feschotte and Eggimann reinvestigated the Ni/Ga system[15] and obtained for '$NiGa_4$' a lattice parameter $a = 8.424$ Å, but could not determine the composition of the phase. In an attempt to solve the structure of '$NiGa_4$', Jingkui and Sishen distributed 8 Ni and 32 Ga atoms on four different crystallographic sites in the space group $I23$ (refined lattice parameter $a = 8.4295$ Å).[16] The total atomic arrangement corresponded to the Ir_3Ge_7 structure type, with one set of Ga atoms occupying the Ir site and the Ni atoms partly occupying one of the two Ge sites. For the phase '$PdIn_3$' no detailed structural analysis has been reported. In the most recent investigation of the Pd/In system Harris et al. obtained a lattice parameter $a = 9.4144$ Å for the phase '$PdIn_3$' with the 'γ-brass structure'.[17] Both phases are reported to decompose peritectically into a mixture of T_2E_3 (Ni_2Al_3 type) and E. The decomposition temperature of '$NiGa_4$' (Ni_3Ga_7) is 358 °C[15] and that of '$PdIn_3$' (Pd_3In_7) 664 °C.[18]

According to our investigations the phases '$NiGa_4$' and '$PdIn_3$' are in fact the compounds Ni_3Ga_7 and Pd_3In_7 with the Ir_3Ge_7 structure. The lattice parameters of Ni_3Ga_7 ($a = 8.4285(6)$ Å) and Pd_3In_7 ($a = 9.4323(2)$ Å) correspond to those reported for '$NiGa_4$' and '$PdIn_3$'. EDX analyses on numerous crystallites in our Ni/Ga and Pd/In samples never revealed any statistically significant deviations from the composition T_3E_7. Thus, we conclude that Ni_3Ga_7 and Pd_3In_7 represent the most E-rich compounds in their respective systems.

2. The Ir_3Ge_7 structure type

2.1 Geometrical analysis: The body-centred cubic Ir_3Ge_7 structure type was first discovered by O. Nial for the crystal structure of the compounds Ru_3Sn_7 and Ir_3Sn_7.[19,20] It consists of only three independent atomic positions, one for the T atoms and two for the E atoms (E1 and E2). Up till now 25 compounds with the composition T_3E_7 have been reported to adopt this structure type, but only for 12 of them have atomic parameters been determined.[21] The refined atomic positions and isotropic displacement factors for the representatives Ni_3Ga_7 and Pd_3In_7 investigated by us are listed in Tables 4 and 5, and in Table 6 the relevant atomic distances are given.

In the Ir_3Ge_7 structure the T atoms sit at the centre of square antiprisms formed by the E atoms, and an ensemble of two condensed antiprisms sharing a square face represents the fundamental building unit of this structure type (Figure 1a).

Table 4. Atomic coordinates, occupancies and displacement parameters (10^4 Å^2) for Ni_3Ga_7.

Atom	Site	x	y	z	SOF[a]	U_{iso}
Ni	12e	0.35050(8)	0	0	1	78(1)
Ga1	12d	1/4	0	1/2	1	155(2)
Ga2	16f	0.16121(4)	x	x	1	107(1)
	U_{11}	U_{22}	U_{33}	U_{12}	U_{13}	U_{23}
Ni	77(2)	79(2)	79(2)	0	0	0
Ga1	74(2)	196(2)	196(2)	0	0	0
Ga2	107(1)	107(1)	107(1)	6(1)	6(1)	6(1)

[a] SOF = site occupancy factor.

Table 5. Atomic coordinates, occupancies and displacement parameters (10^4 Å^2) for Pd_3In_7.

Atom	Site	x	y	z	SOF	U_{iso}
Pd	12e	0.34819(3)	0	0	1	76(1)
In1	12d	1/4	0	1/2	1	128(1)
In2	16f	0.16219(2)	x	x	1	102(1)
	U_{11}	U_{22}	U_{33}	U_{12}	U_{13}	U_{23}
Pd	68(1)	80(1)	80(1)	0	0	0
In1	60(1)	162(1)	162(1)	0	0	0
In2	102(1)	102(1)	102(1)	11(4)	11(4)	11(4)

Table 6. Selected bond lengths [Å] in Ni_3Ga_7 and Pd_3In_7. The standard deviations are all equal to or less than 0.001 Å.

Ni – Ga1	2.455 × 4	Pd – In1	2.759 × 4
Ni – Ga2	2.498 × 4	Pd – In2	2.785 × 4
Ni – Ni	2.520 × 1	Pd – Pd	2.864 × 1
Ga1 – Ni	2.455 × 4	In1 – Pd	2.759 × 4
Ga1 – Ga1	2.980 × 4	In1 – In1	3.335 × 4
Ga1 – Ga2	3.250 × 8	In1 – In2	3.630 × 8
Ga2 – Ni	2.498 × 3	In2 – Pd	2.785 × 3
Ga2 – Ga2	2.592 × 1	In2 – In2	2.869 × 1
Ga2 – Ga2	2.718 × 3	In2 – In2	3.060 × 3
Ga2 – Ga1	3.250 × 6	In2 – In1	3.630 × 6

The rotation angle between the square faces of the antiprisms is independent of the E atom parameters and is always 45°. Thus the point group symmetry of the barrel-shaped building unit is D_{4h}. The E atoms situated at the waist of the barrel (the shared square face) are denominated E1 atoms and those defining the opposite square faces correspond to E2 atoms. The barrels are joined together to a framework by sharing common edges of the terminal square faces in such a way that a cube is formed as a junction unit (Figure 1b). The centres of these empty cubes represent the corners of the unit cell and the resulting framework is topologically equivalent to the arrangement of unit cell edges in a simple cubic structure. A second equivalent framework is generated by the I symmetry of the lattice (Figure 1c). The two interpenetrating frameworks share the same E1 atoms, which occupy the high-symmetry special position 12d (1/4, 0, 1/2).

The topology of the interpenetrating frameworks in the Ir_3Ge_7 structure is governed by only one variable, namely the x parameter of the site 16f (x, x, x) occupied by the E2 atoms. This parameter can theoretically range from 0 to 1/4 and determines the size of the empty cubes centred at 2a (0, 0, 0). The size of the cubes is largest for x_{E2} values close to 1/4. Four different distances characterise the E atom substructure: the

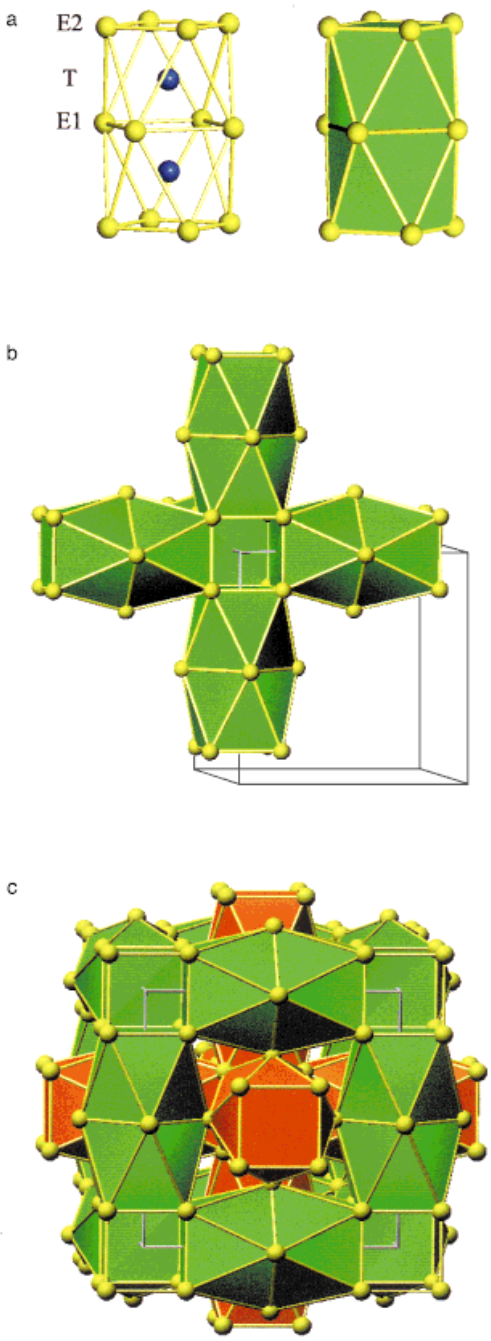

Figure 1. The Ir_3Ge_7 structure type: a) the central building unit consisting of two face-condensed square antiprisms; b) linkage of the building units to a single framework in Ir_3Ge_7; c) the complete structure of Ir_3Ge_7 built of two interpenetrating frameworks of the type shown in b.

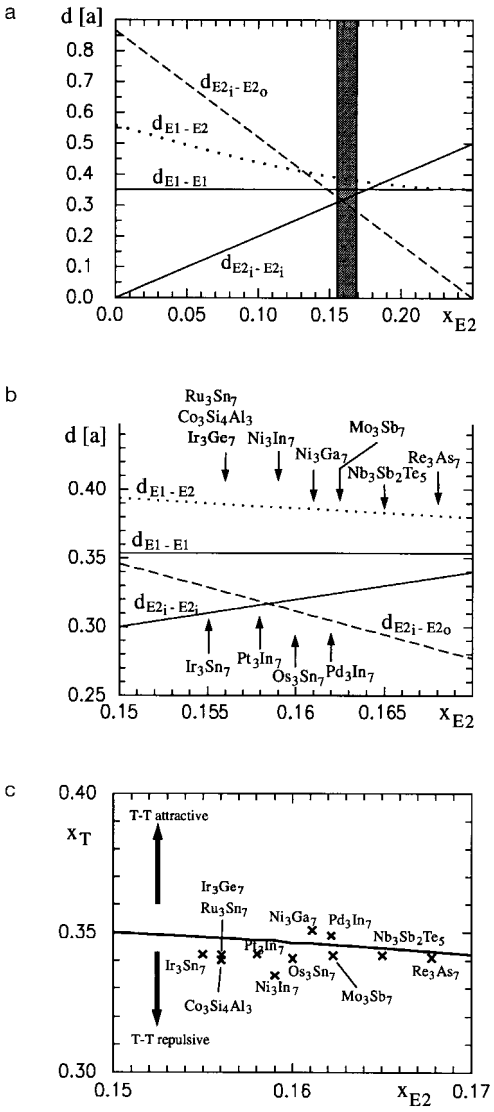

Figure 2. a) The four different distances between Ge (E) atoms in the Ir_3Ge_7 structure as a function of the atomic parameter x_{E2}. The region where the actual values of the known compounds are situated is marked. b) Enlargement of the section marked in (a). The x_{E2} values of the representatives with determined atomic parameters are indicated with arrows. c) The relation $x_T = (3x_{E2}^2 - 5/16)/(2x_{E2} - 1)$ (solid curve) follows from the condition of equal T–E1 and T–E2 distances in the Ir_3Ge_7 structure type. The pairs x_T/x_{E2} of the known representatives follow this relation. Large x_T values imply short T–T distances.

distance d_{E1-E1} between two E1 atoms (occuring 4 times), the distance d_{E1-E2} between an E1 and an E2 atom ($\times 8$), the distance $d_{E2_i-E2_i}$ between two E2 atoms within a cube ($\times 3$), and finally the distance $d_{E2_i-E2_o}$ between two E2 atoms belonging to neighbouring cubes in different frameworks ($\times 1$). In Figure 2a the four distances are displayed as a function of the x_{E2} parameter. It is easy to recognise that it is not possible to built the E atom framework from idealised square antiprisms ($d_{E1-E1} = d_{E2_i-E2_i} = d_{E1-E2}$) and that one of the E2–E2 distances is always the shortest contact in the E substructure. The actual representatives of the Ir_3Ge_7 type have values for the x_{E2} parameter in the narrow range between 0.155 and 0.169 (Figure 2b). In this range the four relevant E–E distances differ least and the distance d_{E1-E2} is always largest.

The second structural variable of the Ir_3Ge_7 type is the x parameter of the site 12e (x, 0, 0) occupied by the T atoms. This parameter determines the distance between the pair of T atoms in the building unit and the distance between T and E1 atoms. Like the values for the x_{E2} parameter also the ones for the x_T parameter are found in a narrow range ($0.334 < x_T < 0.353$). If one assumes strong T–T bonding or repulsive interaction in a single building block one would expect the two kinds of distances between T and E atoms to become

© WILEY-VCH Verlag GmbH, D-69451 Weinheim, 1998
0947-6539/98/0406-1010 $ 17.50+.50/0 *Chem. Eur. J.* **1998**, *4*, No. 6

distinctly different. The condition $d_{T-E1} = d_{T-E2}$ leads to the following relation between the two structural variables of the Ir_3Ge_7 type: $x_T = (3x_{E2}^2 - 5/16)/(2x_{E2} - 1)$. Figure 2c displays this relation together with the pairs x_T/x_{E2} of the representatives and it is clearly seen that the compounds adapt very well to the condition for equal T–E distances. From this geometrical analysis we conclude that, for the compounds with the Ir_3Ge_7 structure type, T–E bonding interactions should be favoured over T–T bonding interactions and that d_{E1-E2} as the largest relevant E–E distance is most probably of minor bonding significance. In the next section we try to investigate in more detail the bonding properties and structural stability of the Ir_3Ge_7 structure type.

2.2. Analysis of the chemical bonding

General aspects: Figure 3 summarises the compounds with the Ir_3Ge_7 structure type together with their valence electron concentration (VEC, number of valence electrons per formula unit). The T component is preferentially represented by

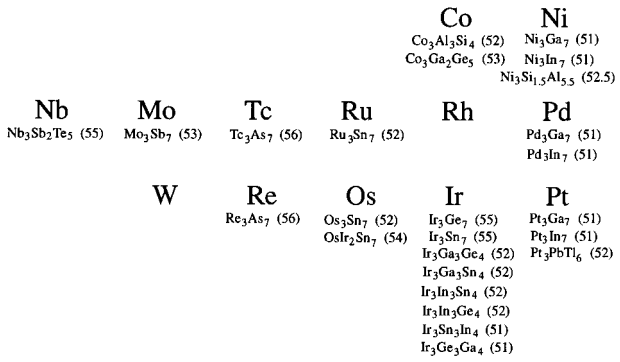

Figure 3. Summary of the known compounds with the Ir_3Ge_7 structure type. The figures in parentheses are the VECs.

4d and 5d transition metals and the E component by the triels Ga and In, the tetrels Ge and Sn, and the pentels As and Sb. Inspecting the pairs T/E, one observes the tendency of the electron-poor transition metals with seven or fewer valence electrons to combine with electron-rich pentels, the tendency of the transition metals with eight or nine valence electrons to combine with tetrels, and the tendency of the transition metals with 10 valence electrons to combine with triels. This restricts the range of VEC to values between 51 and 56 electrons per formula unit for the compounds with the Ir_3Ge_7 structure.

Interestingly, some of the pentel-containing compounds were reported to be semiconductors. First Hulliger found semiconducting behaviour of Re_3As_7 from resistivity measurements,[22] a result which was questioned by Jensen et al.[23] Later Jensen and Kjekshus prepared a compound $Nb_3Sb_2Te_5$ and proposed it as a semiconductor.[24]

The following analysis of the chemical bonding is performed in three steps and addresses the role of VEC for the structural stability of the Ir_3Ge_7 type as well as the electrical conductivity properties of its representatives.

Analysis of the electron localisation function (ELF): bonding topology: In order to attain an overview of the bonding situation connected with the Ir_3Ge_7 type we computed the ELF[25] from the total densities of the compounds Mo_3Sb_7, Ir_3Ge_7, Ru_3Sn_7 and Ni_3Ga_7. The scalar function ELF has developed into a powerful tool for the characterisation of bonds in molecules and solids[26,27] by visualisation of the Pauli repulsion in these fermionic systems.[28] The function is normalised to the interval between 0 and 1. Large values indicate regions in space where the Pauli repulsion is small, that is, where two electrons with antiparallel spin are likely to be paired, and conversely the ELF adopts small values in regions between electron pairs. The local maxima of the ELF are called localisation attractors and are classified as either bonding or nonbonding in the valence region.[29] A bonding attractor is located between two or sometimes more atomic cores whereas a nonbonding attractor, usually associated with a lone pair of electrons, belongs to only one atomic core. The atomic cores and bonding attractors characterise the bonding topology of a molecule or a solid, and from the resulting bonding diagrams[29] it is possible to assign bonds between groups of atoms. It is important to note that this assignment of bonds on the basis of the ELF is independent of the kind of method, basis set and orbitals used for the construction of the many-electron wave function.

When defining a bond between a pair of atoms by a single ELF attractor located between the cores, the internuclear distance is crucial for the formation of such a bond. The onset of a bonding attractor will only be observed when the internuclear distance is below a certain value and, importantly, a *bonding interaction* between two atoms as extracted from atomic orbital interactions in LCAO-MO theory usually occurs at larger internuclear distances. For intermetallic compounds it is characteristic that the number of localisation attractors by far exceeds that of electron pairs possible in principle. Therefore it is in general not possible to assign localised orbitals to the bond-defining attractor regions. These so-called unsaturated attractors[29] indicate complex multicentre bonding or delocalised bonding in the LCAO-MO language.

Coming back to the Ir_3Ge_7 type, the essential information is obtained by calculating and analysing the ELF in the planes (100) and (110). The (100) planes contain the pairs of T and the squares of E1 atoms (that is the distance d_{E1-E1}) and bisect the line $d_{E2_i-E2_i}$ (see Figure 1c). The (110) planes bisect the cubes formed by the E2 atoms along their face diagonals and thus contain, besides the pairs of T atoms, the distances $d_{E2_i-E2_i}$ and $d_{E2_i-E2_o}$ (Figure 1c). In the two-dimensional representations the ELF is displayed with contour lines and colour-coded together with the electron density. The colour code is analogous to a map in which regions of high ELF values are coloured orange–white and regions of low values blue–violet. In Figure 4a the ELF for Mo_3Sb_7 as a representative for compounds with pentels as the E component is shown. (The localisation pattern for Re_3As_7 is very much alike.) The regions of highest localisation in this compound occur between Mo and Sb1 atoms, and Mo and Sb2 atoms. Additional bonding attractors are found between the pairs of Mo atoms and the pairs of Sb2 atoms belonging to different frameworks ($Sb2_i$–$Sb2_o$). The localisation attractors associated with the second kind of Sb2–Sb2 pairs, which form the

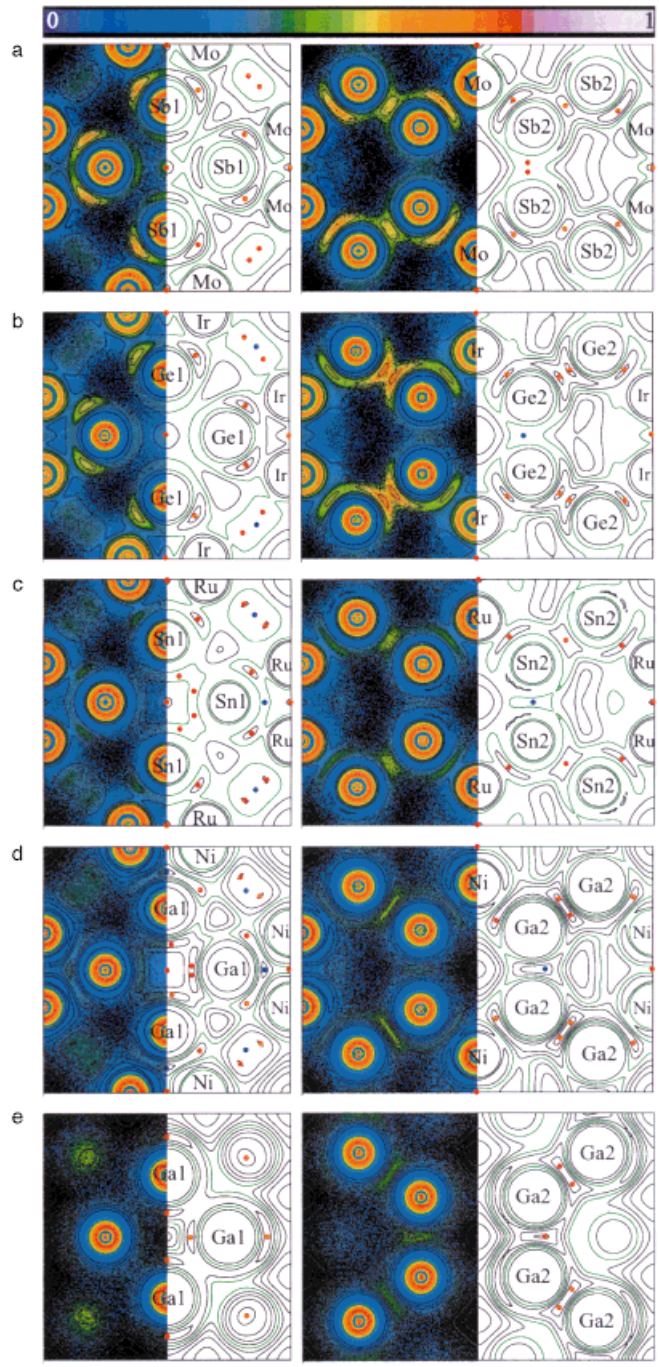

Figure 4. ELF sections (based on LMTO calculations) of the planes (100) (left) and (110) (right) in the compounds a) Mo_3Sb_7, b) Ir_3Ge_7, c) Ru_3Sn_7 d) Ni_3Ga_7 and e) in the Ga substructure in Ni_3Ga_7 without Ni atoms ('Ga_7'). The separation of the contours in a – c is 0.1 and the contour ELF = 0.3 is drawn in green. The separation of the contours in d,e is 0.05 and the contour ELF = 0.25 is drawn in green. The positions of the attractors (ELF maxima) are marked with red circles; some saddle points are marked with blue circles.

cubes in a single framework ($Sb2_i - Sb2_i$), represent a special situation. In the (100) plane a broadened area of higher ELF values is recognisable in the region where $d_{Sb2_i-Sb2_i}$ is bisected. This area perpendicular to the pair $Sb2_i - Sb2_i$ contains two attractors, a phenomenon which is usually observed in π-bonded systems. However, the (110) plane reveals not a single saddle point between this atomic pair, as expected as a consequence of the two maxima in the (100) plane, but two more maxima. All together four attractors are connected with the distance $d_{Sb2_i-Sb2_i}$, but their arrangement is not compatible with a bond between this pair of Sb2 atoms. In contrast, in Ir_3Ge_7 (Figure 4b) a bond can be assigned between the pair of atoms $Ge2_i - Ge2_i$ whereas between the pair $Ge2_i - Ge2_o$ two nonbonding attractors appear. In Ru_3Sn_7, bonds are found between both kinds of E2 atom pairs (Figure 4c). Further, in Ru_3Sn_7 the maxima associated with the T – T bonds are not very pronounced with respect to the surrounding saddle points where ELF isosurfaces of neighbouring localisation domains merge[30] and a new type of attractor emerges (Figure 4c, left). These attractors are situated above and below a triangle Ru-Sn1-Ru and thus cannot be assigned to a particular pair of atoms. In Ni_3Ga_7 this new kind of attractor is even more pronounced whereas the attractors associated with the pairs T – T and T – E1 become hardly recognisable (Figure 4d, left). Interestingly, when the ELF for the Ga substructure is calculated, only the (100) plane reveals a nonbonding attractor, which is located at the position of the saddle point between the Ni-Ga1-Ni maxima in the complete Ni_3Ga_7 structure (Figure 4e, left). On the other hand bonding attractors are found between the two different pairs of Ga2 atoms, and the bonding topologies for the Ga2 substructures in Ni_3Ga_7 and the hypothetical Ga substructure without Ni atoms correspond to each other (Figures 4d,e right).

From the analysis of the ELF we observe that the bonding picture within the Ir_3Ge_7 structure can change dramatically. Mo_3Sb_7 and Re_3As_7 are characterised by pronounced bonds between pairs of T and pairs of T and E atoms. From Ir_3Ge_7 and Ru_3Sn_7 to Ni_3Ga_7 the T – T and T – E bonds become less and less well-defined when comparing the differences of the maxima and the surrounding saddle points. Instead the substructure of E2 atoms emerges, corresponding to a bcc arrangement of cubes with well-defined bonds.

Analysis of the band structures: The investigation of the ELF represents a real-space bonding analysis; in order to obtain a complete view of the bonding situation in compounds with the Ir_3Ge_7 type, information from their band structures is also essential. In the following we discuss the density of states (DOS), which represents the one-dimensional projection of a band structure, of the compounds Mo_3Sb_7, Ru_3Sn_7 and Ni_3Ga_7. Figure 5 depicts the DOS distributions obtained from TB-LMTO-ASA calculations for the three compounds.

The DOS of Mo_3Sb_7 is characterised by two gaps and is thus split into three different parts. The part lowest in energy represents the Sb s bands and is occupied by 14 electrons per formula unit. Therefore the Sb s orbitals do not contribute to the bonding in Mo_3Sb_7. The second part of the DOS can be broken into contributions from the Mo d and Sb p orbitals with the Mo d partial DOS distributed over the complete energy range between − 5.5 and 0.5 eV. This indicates that the Mo d orbitals participate in dispersive bands which are a consequence of strongly bonding interactions with the Sb p orbitals. The second gap, about 0.8 eV wide, corresponds to a band filling of 55 electrons per formula unit and is just above the Fermi level of Mo_3Sb_7 (VEC = 53). This gap is a direct consequence of the strong dp bonding, which can be seen by

© WILEY-VCH Verlag GmbH, D-69451 Weinheim, 1998
0947-6539/98/0406-1012 $ 17.50+.50/0 *Chem. Eur. J.* **1998**, *4*, No. 6

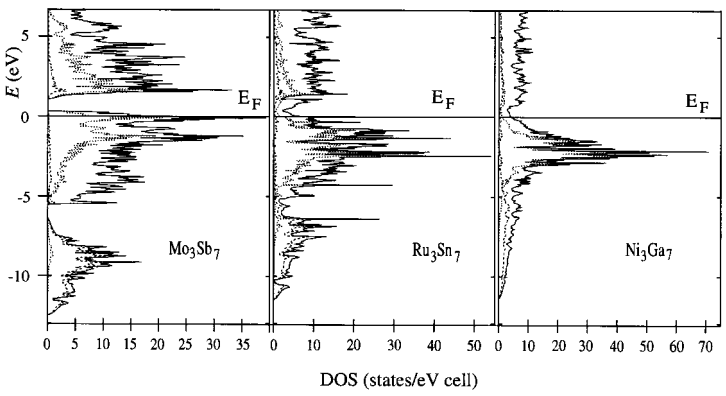

Figure 5. Total density of states (DOS) together with the T d (dotted lines) and E s orbital contributions (dashed lines) of the compounds Mo_3Sb_7, Ru_3Sn_7, and Ni_3Ga_7 from LMTO calculations (primitive unit cell).

the symmetrical distribution of the Mo d partial DOS below and above this second gap. Above the gap the states are strongly Mo–Sb (dp) antibonding. In Re_3As_7, which has the same structuring of the DOS a few of these antibonding states are already occupied because the VEC is 56. Thus Re_3As_7 is a metallic conductor and the questioning of Hulliger's results concerning the conductivity properties of Re_3As_7 by Jensen et al. appears to be justified.[22,23] However, there is the possibility that, due to different synthesis conditions, Hulliger obtained an As-deficient compound $Re_3As_{6.8}$ with the appropriate VEC of 55. The compound $Nb_3Sb_2Te_5$ has this VEC.[24]

Strong dp-bonding interactions require the diffuse d orbitals of the earlier transition metals from the second and third transition series. As the nuclear charge increases, the d orbitals of these metals become more contracted [31] (note that compared with 4d and 5d orbitals, 3d orbitals are much more contracted). Thus the dp orbital interactions diminish gradually and sp-bonding interactions between the E atoms become more important. As a consequence both band gaps are expected to diminish and, indeed, they are already closed in the DOS of Ru_3Sn_7 (VEC = 52). Note how much the DOS of Ru_3Sn_7 resembles that of Mo_3Sb_7. The three different parts are still recognisable but the Ru d orbital contribution to the states below the Fermi level is considerably larger. In Ni_3Ga_7 (VEC = 51) Ga s and p orbitals mix completely and the Ni d orbitals give rise to a large contribution to the DOS in the narrow energy range between -1 and -3 eV. Thus the d orbitals interact only very weakly with the orbitals of E, which gives rise to flat, nonbonding bands. All the d-based bands are now occupied; that is, the DOS above the Fermi level has very little Ni d orbital contribution.

The results from the analysis of the band structure/DOS correspond exactly to those obtained from analysis of the ELF: The Ir_3Ge_7 structure type can accomodate two extreme forms of bonding motifs. In the case of strong dp orbital interactions, a band gap at VEC = 55 is opened and bonds are formed between pairs of T–E and T–T atoms as well as between the pairs of E2 atoms belonging to different frameworks. In the case of weak dp orbital interactions, the sp-bonded substructure of E2 atoms corresponding to a bcc arrangement of cubes becomes important and bonds are found between the pairs of E2 atoms forming the cubes and the pairs of E2 atoms between cubes belonging to different frameworks.

We want to conclude our analysis of the chemical bonding by addressing the role of the VEC in the structural stability of the Ir_3Ge_7-type compounds.

VEC and structural stability: The known compounds with the Ir_3Ge_7 structure exist in the narrow range of VEC between 51 and 56 electrons per formula unit. In order to investigate the role of VEC for the stability of those compounds we calculated the crystal orbital overlap population (COOP) curves for Mo_3Sb_7 and Ni_3Ga_7 with the tight-binding extended Hückel method. In Figure 6a the DOS and COOP curves for Mo_3Sb_7 are shown. The total DOS obtained from the semiempirical calculation is in perfect agreement with that obtained from the ab inito calculation (Figure 5) and also the distribution of the Sb s and Mo d orbital contributions corresponds exactly. The only difference is that in the semiempirical DOS the Sb s bands are not clearly separated but the second band gap at VEC = 55 appears very pronounced. As anticipated from the considerations in the preceding paragraph, the states below this band gap are strongly Mo–Sb (dp) bonding and those above strongly antibonding. For the calculation of the Sb–Sb COOP curve all four different Sb–Sb contacts (see Figures 2 a,b) have been taken into account. The Sb–Sb orbital interactions appear as partly bonding and partly antibonding, and one notes that despite these opposite interactions, a bond between $Sb2_i$ and $Sb2_o$ atoms is observed when analysing the ELF. For compounds with strong dp bonding the optimum VEC should be 55, but small deviations as observed in Mo_3Sb_7 (VEC = 53) and Re_3As_7 (VEC = 56) are apparently tolerated.

Why do the compounds with weak dp bonding adopt a similar VEC? In Figure 6b we show the DOS and COOP curves for Ni_3Ga_7 (VEC = 51) and again the agreement between semiempirical and ab initio DOS is very good (cf. Figure 5). When collating the COOP curves of Mo_3Sb_7 and Ni_3Ga_7 a crucial difference is recognised: In Ni_3Ga_7 the Ga–Ga (sp) orbital interactions are strongly bonding until the Fermi level is reached. (Note here that also the Ga1–Ga1 interactions are of bonding nature although no bond is formed between these atoms.) To understand the optimum VEC for Ni_3Ga_7 one might consider a sp-bonded Ga substructure in which weakly interacting Ni atoms are embedded. In Figure 6c we compare the partial DOS of the Ga atoms in Ni_3Ga_7 and the DOS of a hypothetical Ga structure without Ni atoms. The curves are in remarkable agreement and deviate only in the region between -11 and -9 eV, where the Ni d orbitals are centred, and in the region above the Fermi level of Ni_3Ga_7. The COOP curve of the hypothetical Ga structure without Ni atoms exhibits a sharp change from Ga–Ga bonding to antibonding interactions at an energy value where VEC corresponds to 21.5 electrons per 'Ga_7' formula unit (marked by a horizontal line in Figure 6c). At almost the same energy value the Ga–Ga interactions become (more slowly) antibonding in the Ni_3Ga_7. This supports the idea that the embedding of the Ni atoms, which introduces contracted,

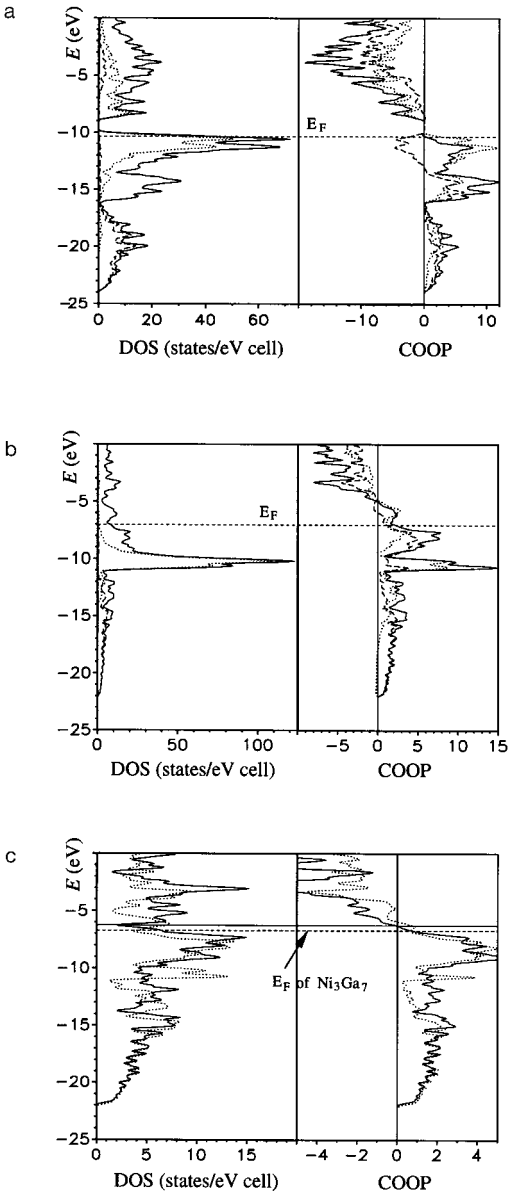

Figure 6. Results from the tight-binding extended Hückel calculations (I-centred unit cell). Left: total density of states (DOS) together with the T d (dotted lines) and E s (dashed lines) contributions of a) Mo_3Sb_7 and b) Ni_3Ga_7; c) the partial DOS of the Ga atoms in Ni_3Ga_7 (dotted line) and the DOS of the Ga substructure in Ni_3Ga_7 without Ni atoms (solid line). Right: crystal orbital overlap population (COOP; solid lines) of the contacts T–E ($4\times$T–E1, $4\times$T–E2; dotted lines) and E–E ($4\times$E1–E1, $8\times$E1–E2, $4\times$E2–E2; dashed lines) in a) Mo_3Sb_7 and b) Ni_3Ga_7; c) the COOP of the contacts Ga–Ga in Ni_3Ga_7 (dotted line) and the Ga substructure in Ni_3Ga_7 without Ni atoms (solid line).

weakly interacting d orbitals, does not dramatically change the electronic structure of the Ga matrix. These d orbitals are occupied by the Ni valence electrons; the optimum VEC for Ni_3Ga_7 approximated as a system consisting of an sp-bonded Ga matrix (with an optimum VEC of 21.5) and noninteracting Ni atoms would be 51.5. This value is only slightly below that for the optimum VEC of strongly dp-bonded compounds. However, the COOP curves of Figure 6b reveal that above the Fermi level of Ni_3Ga_7 a few Ni–Ga bonding states are created and the VEC corresponding to all bonding states occupied increases to 54.

Concluding Remarks

We investigated in detail the chemical bonding properties associated with the remarkable Ir_3Ge_7 structure type. Although the geometrical flexiblity of this structure is rather limited and atomic parameters of the representatives are very similar, we discovered that two extreme bonding motifs can be expressed with the Ir_3Ge_7 type. When the dp orbital interaction is strong, bonding within the single building unit T_2E_{12} consisting of two face-condensed square antiprisms is primary and the DOS exhibits a band gap at or close to the Fermi level. In the case of weak dp orbital interactions an sp-bonded substructure formed by one kind of E atom becomes important. A combination of real and reciprocal space bonding analysis was found to be very useful in the identification of these essential bonding motifs. Interestingly, a VEC of 52–55 is compatible with both bonding motifs and the Ir_3Ge_7 structure is an instructive example of the bonding flexibility characteristic of intermetallic compounds.

The possibility that semiconductors of the Ir_3Ge_7 type may be accessible deserves special attention. Hitherto among the Ir_3Ge_7-type representatives only $Nb_3Se_2Te_5$ and possibly an As-deficient Re_3As_7 fulfil the two conditions for semiconductivity, namely strong dp bonding (for the opening of the band gap) and an appropriate VEC of 55 electrons per formula unit. In principle it should be possible to synthesise ternary and quaternary representatives of the Ir_3Ge_7 type and obtain the proper VEC by the flexible ratio of two different kinds of T atoms and/or two different kinds of E atoms. Such elemental variations might even make it possible to tune the width of the band gap or create metal–insulator transitions.

Acknowledgements: This work was supported by the Swedish National Science Research Council (NFR) and the Crawfoord Foundation.

Received: December 10, 1997 [F921]

[1] B. Eisenmann, G. Cordier in *Chemistry, Structure and Bonding of Zintl Phases and Ions* (Ed.: S. M. Kauzlarich), VCH, New York, **1996**, pp. 61–137 and references therein.
[2] J. D. Corbett, *Chemistry, Structure and Bonding of Zintl Phases and Ions* (Ed.: S. M. Kauzlarich), VCH, New York, **1996**, pp. 139–181 and references therein.
[3] a) H. Schäfer, B. Eisenmann, W. Müller, *Angew. Chem.* **1973**, *85*, 742; *Angew. Chem. Int. Ed. Engl.* **1973**, *12*, 694; b) H. Schäfer, *Annu. Rev. Mater. Sci.* **1985**, *15*, 1; c) R. Nesper, *Prog. Solid-State Chem.* **1990**, *20*, 1; d) C. Belin, M. Tillard-Charbonell, *ibid.* **1993**, *22*, 59.
[4] Siemens Analytical X-Ray Instruments, *SMART Reference Manual*, Madison, Wisconsin (USA), **1996**.
[5] Siemens Analytical X-Ray Instruments, *ASTRO and SAINT: Data Collection and Processing Software for the SMART System*, Madison, Wisconsin (USA), **1995**.
[6] G. M. Sheldrick, *SADABS User Guide*, University of Göttingen, Göttingen (Germany), **1996**.
[7] G. M. Sheldrick, *SHELXL-93 Program for the Refinement of Crystal Structures*, University of Göttingen, Göttingen (Germany), **1993**.
[8] M. van Schilfgarde, T. A. Paxton, O. Jepsen, G. Krier, A. Burkhard, O. K. Andersen, *Program TB-LMTO 4.6*, Max-Planck-Institut Stuttgart, Stuttgart (Germany), **1994**.
[9] U. von Barth, L. Hedin, *J. Phys. C* **1972**, *5*, 1629.
[10] G. Krier, O. K. Andersen, O. Jepsen, unpublished results.
[11] O. Jepsen, O. K. Andersen, *Solid-State Commun.* **1971**, *9*, 1763.
[12] M. H. Whangbo, M. Evain, T. Hughbanks, M. Kertesz, S. Wijeyesekera, C. Wilker, C. Zheng, R. Hoffmann, *Program EHMACC:*

© WILEY-VCH Verlag GmbH, D-69451 Weinheim, 1998

Extended Hückel Molecular and Crystal Calculations; Program EHPC: Extended Hückel Property Calculations, QCPE Version, **1987**; U. Häussermann, R. Nesper, S. Wengert, T. F. Fässler, *Program MEHMACC: modified extended Hückel version based on EHMACC*, ETH Zürich, Zürich, **1994**. MEHMACC additionally allows the self-consistent charge iteration of atomic H_{ii} parameters and the calculation of the electron density, partial electron density and electron localisation function.

[13] E. Hellner, F. Laves, *Z. Naturforschung A* **1947**, *2A*, 177.
[14] E. Hellner, *Z. Metallk.* **1950**, *41*, 480.
[15] P. Feschotte, P. Eggimann, *J. Less-Common Met.* **1974**, *63*, 15.
[16] L. Jingkui, X. Sishen, *Scientia Sinica* **1983**, *26*, 1305.
[17] I. R. Harris, M. Norman, A. W. Bryant, *J. Less-Common Met.* **1968**, *16*, 427.
[18] J. R. Knight, D. W. Rhys, *J. Less-Common Met.* **1959**, *1*, 292.
[19] a) O. Nial, *Inaugural Dissertation*, University of Stockholm, **1945**; b) O. Nial, *Svensk Kemisk Tidskrift* **1947**, *59*, 165.
[20] Ru_3Sn_7 and Ir_3Sn_7 are the first phases published of an oversight structure type;[19] however, the Ir_3Ge_7 of O. Nial's work led to the identification of Ir_3Ge_7 as the first representative of this structure type.
[21] P. Villars, L. D. Calvert, *Pearson's Handbook of Crystallographic Data for Intermetallic Compounds*, 2nd ed., ASM International, Ohio, **1991**.
[22] F. Hulliger, *Nature* **1966**, *209*, 500.
[23] P. Jensen, A. Kjekshus, T. Skansen, *J. Less-Common Met.* **1969**, *17*, 455.
[24] P. Jensen, A. Kjekshus, *J. Less-Common Met.* **1967**, *13*, 357.
[25] A. D. Becke, N. E. Edgecombe, *J. Chem. Phys.* **1990**, *92*, 5397.
[26] A. Savin, A. D. Becke, J. Flad, R. Nesper, H. Preuss, H. G. von Schnering, *Angew. Chem.* **1991**, *103*, 421; *Angew. Chem. Int. Ed. Engl.* **1991**, *30*, 409.
[27] A. Savin, O. Jepsen, J. Flad, O. K. Andersen, H. Preuss, H. G. von Schnering, *Angew. Chem.* **1992**, *104*, 186; *Angew. Chem. Int. Ed. Engl.* **1992**, *31*, 187.
[28] T. F. Fässler, A. Savin, *Chem. Unserer Zeit* **1997**, *31*, 110.
[29] A. Savin, B. Silvi, *Nature* **1994**, *371*, 683.
[30] D. Marx, A. Savin, *Angew. Chem.* **1997**, *109*, 2168; *Angew. Chem. Int. Ed. Engl.* **1997**, *36*, 2077.
[31] J. E. Huheey, E. A. Keiter, R. L. Keiter, *Inorganic Chemistry: Principles of Structure and Reactivity*, 4th ed., Harper Collins College, New York, **1993**.

 © WILEY-VCH Verlag GmbH, D-69451 Weinheim, 1998 0947-6539/98/0406-1015 $ 17.50+.25/0